Nanoscale elastic inhomogeneity of a Pd-based metallic glass: Sound velocity from ultrasonic and inelastic x-ray scattering experiments

AUTHOR(S):

Ichitsubo, T.; Hosokawa, S.; Matsuda, K.; Matsubara, E.; Nishiyama, N.; Tsutsui, S.; Baron, A. Q. R.

CITATION:

Ichitsubo, T. ...[et al]. Nanoscale elastic inhomogeneity of a Pd-based metallic glass: Sound velocity from ultrasonic and inelastic x-ray scattering experiments. PHYSICAL REVIEW B 2007, 76(14): 140201.

ISSUE DATE:

2007-10

URL:

http://hdl.handle.net/2433/84626

PHYSICAL REVIEW B **76**, 140201(R) (2007)

Nanoscale elastic inhomogeneity of a Pd-based metallic glass: Sound velocity from ultrasonic and inelastic x-ray scattering experiments

T. Ichitsubo,[1,*] S. Hosokawa,[2] K. Matsuda,[1] E. Matsubara,[1] N. Nishiyama,[3] S. Tsutsui,[4] and A. Q. R. Baron[4,5]
[1]*Department of Materials Science and Engineering, Kyoto University, Kyoto 606-8501, Japan*
[2]*Center for Materials Research using Third-Generation Synchrotron Radiation Facilities, Hiroshima Institute of Technology, Hiroshima 731-5193, Japan*
[3]*RIMCOF, R&D Institute of Metals and Composites for Future Industries, Sendai 980-8577, Japan*
[4]*SPring-8/JASRI 1-1-1 Kouto, Sayo-cho, Hyogo-ken, 679-5198, Japan*
[5]*SPring-8/RIKEN 1-1-1 Kouto, Sayo-cho, Hyogo-ken, 679-5148, Japan*
(Received 11 August 2007; published 16 October 2007)

In this paper, we show experimentally that the sound velocity of nanometer wavelength exceeds that of millimeter wavelength for a Pd-based metallic glass completely frozen far below the glass transition temperature. This indicates that nanoscale elastically harder regions exist in the glass matrix and, hence, elastically softer regions are also present so as to realize the macroscopic elasticity.

DOI: 10.1103/PhysRevB.76.140201 PACS number(s): 61.43.Fs, 62.65.+k, 64.70.Pf, 81.05.Kf

Structural investigation of frozen glass-forming liquids is one of the attractive subjects of present research in glass science. In terms of thermodynamics, rheology, fragility, mechanical response, etc., there are several structural models of glasses.[1–7] In these models, the intrinsic structural fluctuation in a glass substance is explicitly taken into consideration. In contrast, structural investigations by transmission electron microscopy and x-ray diffraction techniques show little evidence of apparent inhomogeneity, except for very recent works.[8,9] In order to reveal nanoscale inhomogeneity, we have previously used ultrasound-induced instability phenomena in metallic glasses;[10–13] in that work glasses are crystallized by atomic jumps during the (Johari-Goldstein) β relaxation resonant with a periodic strain field, and the partially crystallized microstructure of the glass is observed using high-resolution transmission electron microscopy. According to that work, the structure of fragile metallic glasses is expected to consist of strongly bonded regions (SBRs) surrounded by weakly bonded regions (WBRs), as shown in Fig. 1(a). If this structural model is correct, it is predicted that sound velocity of nanometer-order wavelength, which mainly represents the elasticity of SBRs, should become faster than that of millimeter-order wavelength, reflecting the macroscopic elastic stiffness of the overall substance including SBRs and WBRs, although the long-wavelength wave in a homogeneous solid is usually the fastest. To obtain these sound velocities, two measurement techniques are available: inelastic x-ray scattering (IXS) method for the former sound velocity and ultrasonic (US) measurement for the latter. Actually, inelastic neutron and x-ray scattering have been used so far to investigate the dynamics of disordered materials,[14–17] and especially the IXS technique, utilizing third-generation synchrotron radiation sources, facilitates investigation of phonon dispersion at smaller momentum transfers, small Q, and, therefore, allow us to obtain an accurate sound velocity.[18,19] Around the Q value corresponding to the typical domain size ξ, the phonon-dispersion relation is expected to branch positively and negatively from the US line due to the SBR and WBR elasticities, respectively, as shown in Fig. 1(b). (However, the signal associated with the WBR is probably undetectable because its volume fraction is considered to be small and the signal location is close to the quasielastic peak at low Q regions.)

Our goal is to examine the intrinsic features of the glass

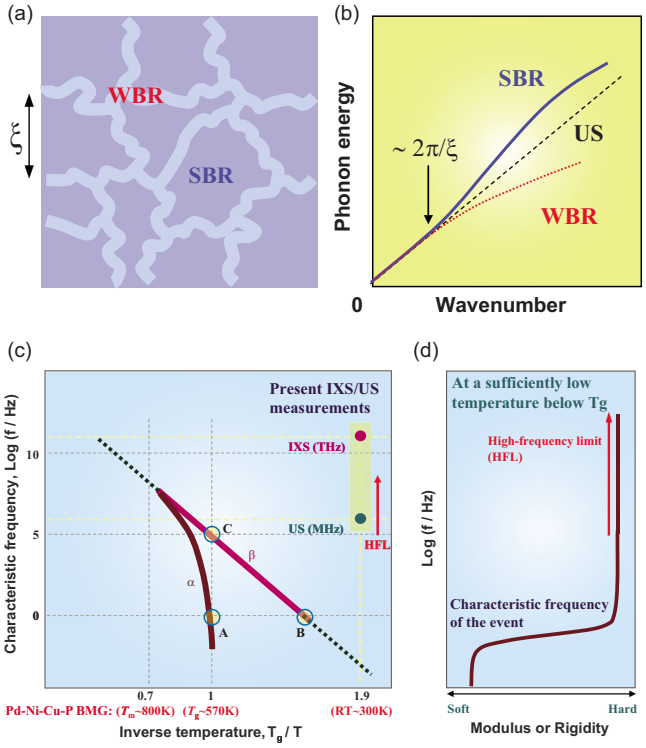

FIG. 1. (Color online) Schematic illustrations showing (a) inhomogeneous structural model of fragile metallic glasses (Ref. 12), (b) phonon dispersion relation in a very small Q region predicted from the model, (c) inverse temperature dependence of the characteristic frequencies of α and β relaxations (referring to Ref. 33), and (d) typical frequency dependence of the modulus or rigidity in a viscoelastic substance. The set of characteristic temperatures in (c) is an example for the case of $Pd_{42.5}Ni_{7.5}Cu_{30}P_{20}$; point A is just the definition of the glass transition, B and C are based on the experiments (Refs. 12, 22, and 23).

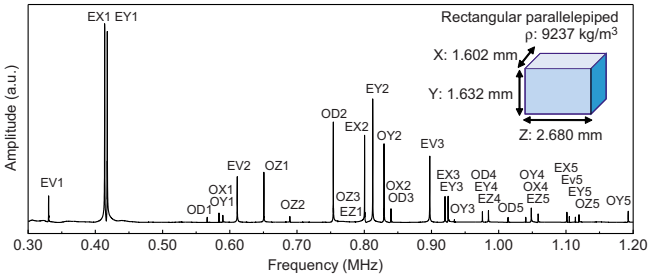

FIG. 2. (Color online) RUS spectrum measured at room temperature for a $Pd_{42.5}Ni_{7.5}Cu_{30}P_{20}$ bulk metallic glass. The inset gives the sample information used in the present RUS measurement. The labeling of the vibrational modes (e.g., EV1, EX1, OD1, etc.) follows Ohno's prescription (Ref. 26). About 40 resonance peaks were used in the inverse analysis, and the root-mean-square error indicating the degree of convergence was about 0.2%. The inverse calculation yields c_{11}=209 GPa and c_{44}=34.2 GPa.

structure by comparing the nanoscopic elasticity to the macroscopic elasticity of a metallic glass, and to show an experimental indication of "nanoscale elastic inhomogeneity." In order to confirm such a "static" structural inhomogeneity, however, we have to eliminate any effects of hardening and softening due to the relaxation processes that frequently appear in glass substances. Thus, in the present work, by using one of the most stable bulk metallic glasses $Pd_{42.5}Ni_{7.5}Cu_{30}P_{20}$,[20] we performed IXS and US measurements at room temperature (about $0.38T_m$ or $0.52T_g$) which is far below the glass transition temperature ($T_g \sim 290-300$ °C).[21] In this metallic system, as shown in Fig. 1(c), it was reported that the β relaxation is observed at about 1 Hz around 150–200 °C,[22] and can also be detected around T_g in the megahertz frequency range.[12,23] This means that any relaxation (except for the residual fast relaxation; this is discussed later) is excluded for ultrasonic (megahertz) measurements at room temperature and, of course, this is also the case for much higher frequencies (terahertz). That is, as is understood from Fig. 1(d) showing the viscoelastic characteristics, the two kinds of sound velocity (US, megahertz; IXS, Terahertz) measured at such a low temperature (e.g., room temperature) are both at the high-frequency limit, so that the velocity difference caused in this situation, if present, is limited only to what is caused by the difference between the wavelengths of the probes (US and IXS). We can therefore discuss the static structure of the glass through the IXS and US dynamic measurements.

First, the longitudinal elastic constant c_L (and also the shear constant c_T) of a rectangular parallelepiped sample cut out of the ingot were determined using the resonant ultrasound spectroscopy (RUS) technique,[25,26] to obtain the longitudinal (and also transverse) US velocity, $v_L^{US}=\sqrt{c_L/\rho}$ (and also $v_T^{US}=\sqrt{c_T/\rho}$). The resonance spectrum was obtained in the range of 0.2–1.5 MHz with steps of 0.1 kHz, and inverse iterative calculations were carried out to determine c_L and c_T from the measured resonance spectrum. Figure 2 shows the resonance spectrum of the sample, from which we have obtained c_L=209 GPa, i.e., v_L^{US}=4.76 km/s, and c_T=34.2 GPa, i.e., v_T^{US}=1.92 km/s. These values are in good agreement with the elastic moduli obtained by other independent measurements: v_L^{US}=4.51 km/s for $Pd_{40}Ni_{10}Cu_{30}P_{20}$ (Ref. 27) and v_L^{US}=4.82 km/s measured for a different sample of $Pd_{42.5}Ni_{7.5}Cu_{30}P_{20}$ glass of the same composition.[23]

A sample cut from the same ingot was mechanically polished into a thin plate with a thickness of about 85 μm appropriate for transmission x-ray measurements. The IXS measurement was performed at the high-resolution IXS beamline BL35XU of SPring-8 in Japan,[24] in a range between 1.5 and 17 nm^{-1}. During the measurement, the $Pd_{42.5}Ni_{7.5}Cu_{30}P_{20}$ plate sample was kept at room temperature in a helium atmosphere. Backscattering at the Si (11 11 11) reflection and an array of 12 analyzers was used, with the best energy resolution 1.6 meV. Scans, at fixed momentum transfer, were performed for energy transfers in the range $-50 \le \hbar\omega \le 50$ meV, and several scans were made to accumulate the data for enhancement of statistical accuracy. After the IXS measurement, the amorphous structure was again confirmed by x-ray diffraction with our laboratory instrument with Mo $K\alpha$ radiation. Figure 3(a) shows the x-ray diffraction profile of the sample before and after the IXS measurement; it was found that the amorphous structure was completely retained after the measurement. Figure 3(b) shows the IXS spectrum at each Q value. The data presented have been corrected for background by subtracting the empty-vessel response, after correction for sample attenuation. The high-energy peaks at low Q values are due to inelastic scattering from the silicon windows of the vessel. In the ideal case, these peaks should be completely removed; the residual intensity in the spectra may come from using only a calculated value for the sample attenuation coefficient. However, these peaks are mostly removed by the background subtraction. Also, as the intensity in the vicinity of the acoustic modes was not very large, this slight deviation does not affect our fundamental result (the inelastic signals from the Si window were masked appropriately for practical analysis). In order to obtain the excitation energy at each Q value, the present IXS spectra were fitted to the damped harmonic oscillator (DHO) function,[28,29]

$$\frac{S(Q,\omega)}{S(Q)} = A_0 \frac{\Gamma_0}{\Gamma_0^2+\omega^2} + A_Q \frac{\Omega_Q^2 \Gamma_Q}{(\omega^2-\Omega_Q^2)^2+\omega^2\Gamma_Q^2}, \qquad (1)$$

where A_0 and A_Q are the relative intensities, Γ_0 and Γ_Q are associated with the sound attenuation, and Ω_Q is the characteristic acoustic frequency that corresponds to the maximum of the current-current correlation spectrum $J(Q,\omega)=(\omega^2/Q^2)S(Q,\omega)$,[18] and, in practice, we included the detailed-balance term and convolved with the instrumental resolution function. Furthermore, since we here put importance on the estimation of the excitation energy in the low Q region, we have remeasured the IXS spectra for Q=1.28 and 1.62 nm^{-1} to enhance the signal-to-noise ratio and to obtain the precise mode energy with a different-thickness sample, which was set in a beryllium-window vessel; see Fig. 3(c). Since, in addition to the primary peak at about 5 meV, a broad faint peak is seen at high energy of about 8 meV in Fig. 3(c), the function including dual (or multiple) DHO terms may be more suitable for fitting to the spectra, but for

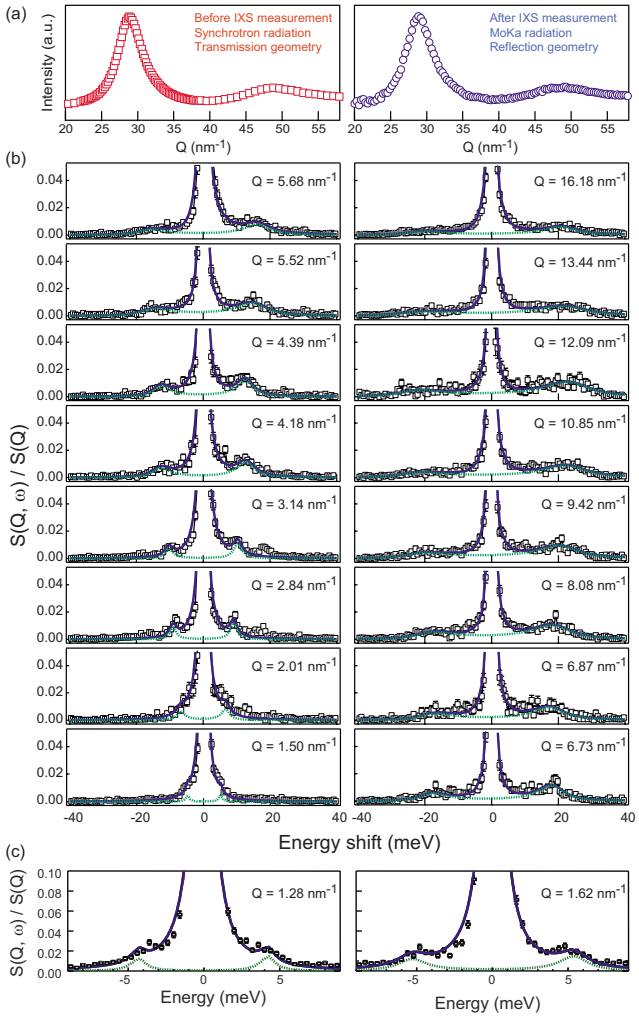

FIG. 3. (Color online) (a) X-ray diffraction profiles of a fresh sample and the sample after the IXS measurement. (b) IXS spectra obtained for $Pd_{42.5}Ni_{7.5}Cu_{30}P_{20}$ at fixed Q values. The high-energy peaks indicated by white squares at low Q values are due to spurious scattering from the silicon windows of the vessel. The blue (solid) and green (dashed) curves indicate the fitted Eq. (1) and the damped terms in Eq. (1), respectively. (c) The refined IXS spectra at very low Q values obtained by the precise measurements performed for a different sample cut from the same ingot, in order to enhance the signal-to-noise ratio by narrowing the slit of the 2θ arm and optimizing the sample thickness.

the sake of simplicity, here we analyze the spectra by using the single-DHO function (this is discussed later). Figure 4 shows the phonon-dispersion relation (upper panel) and compares the phase velocity Ω_Q/Q of longitudinal sound from the IXS data with the US velocities (lower panel). Usually, the US velocity (of $\lambda \sim 1$ mm) in homogeneous solids is substantially equivalent to the fastest sound velocity of long-wavelength limit. However, as found from Fig. 4, the sound velocities in the low Q region are found to be apparently higher than the US velocity in this case. It is found that the velocities at low Q values exceed $v_L^{US}=4.76$ km/s and the difference in $c_L(=\rho v_L^2)$ between IXS and US amounts to 10–20 %. The sound velocity at $Q \approx 4$ nm^{-1} is virtually equal to the US velocity, indicating that the plots at

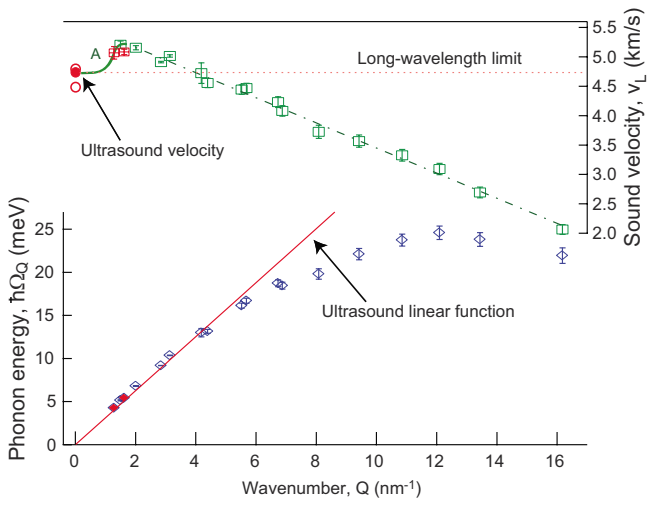

FIG. 4. (Color online) Phonon-dispersion curve obtained from the IXS data for a $Pd_{42.5}Ni_{7.5}Cu_{30}P_{20}$ bulk metallic glass (lower), and comparison of the sound velocity (Ω_Q/Q) of longitudinal sound obtained from the IXS data and the US velocities (upper). The line "Ultrasound linear function" in the lower part denotes $\hbar\Omega_Q=v_L^{US}Q$. The additional two IXS data are also plotted in the figure, and the previous US data (Refs. 23 and 27) are also shown for reference. The sound-velocity plot in the low Q region is considered to be connected to the long-wavelength limit by the curve A depicted in the figure.

$Q<4$ nm^{-1} apparently deviate positively from the US linear function ($\hbar\Omega_Q=v_L^{US}Q$). For consistency, the sound-velocity plots in the low Q region should be connected to the long-wavelength limit as in the curve A depicted in the figure. If we had obtained the critical point deviation from the US line by measuring the excitation energy at Q values less than 1.28 nm^{-1}, we would know the typical domain size ξ in Fig. 1(a). It is emphasized here that the fast sound, v_L (≈ 5.07 km/s $> v_L^{US}$), at $Q=1.28$ nm^{-1}, indicates that ξ is larger than 5 nm.

The present fast-sound tendency is the first data for metallic glasses, but a similar phenomenon was also observed on a simple glass, selenium, and a silica glass.[30,31] The phenomenon has been attributed to residual fast relaxation in the glass and to topological disorder.[31,32] Although it may be one of the candidates for the mechanism, there seems to be no clarity on the issue at present. Based on the energy landscape concept, the dynamics far below T_g is dominated by the potential barriers in a glassy solid state (i.e., in the landscape-dominated regime);[33,34] hence, it might be difficult to suppose that a very fast relaxation process of the order of MHz-THz occurs in a sufficiently frozen glassy solid (at about $0.38T_m$ or $0.52T_g$). Thus, the fact that the sound velocities at nanoscale wavelengths exceed the US velocities close to the long-wavelength limit directly indicates that elastically harder regions exist in the glassy matrix and, therefore, elastically softer regions also exist so as to realize the relatively low elasticity of the overall glass substance. With reference to recent work on the structure of metallic glasses by transmission electron microscopy,[8,9] the present interpretation for the fast sound in rigid glasses is considered to be valid. Such

a structural inhomogeneity strongly supports the idea of Ngai[35] or Johari[36] that not all molecules (atoms) may contribute to the Johari-Goldstein β relaxation process, and also is consistent with the recent papers associated with the elastic inhomogeneity of glasses.[37–42]

Finally, we add some remarks on the peak broadening (or faint splitting) toward the higher-energy region observed in the present IXS data. If the glass structure is composed of two distinct regions, the excitation energies would be split into clear two peaks (in the limit of no damping). But, when the structure is comprised of vague regions whose elasticity changes gradually, the excitation peaks are broadened and, in addition, the damping effect also contributes to the peak broadening. By overlapping of the broad higher-energy peak, the overall peak looks like one faster sound peak as seen in Fig. 3(c). From the trial of dual-DHO analysis, the sound velocity of the lower-energy mode is found to be very close to the US velocity. Here, supposing that the first lower-energy (primary) peak comes from WBRs, the overall elasticity consisting of both SBRs and WBRs inevitably exceeds the average elasticity obtained by US; hence, this assumption is not valid. Usually, the lifetime of excited phonons due to the damping is of (sub)picosecond order; therefore, the propagation length l_{ph} is approximately of the order 1 nm, assuming that the sound velocity is 1000–10 000 m/s. So, when $\xi \geq l_{\mathrm{ph}}$, the faster sound velocity of the SBRs is mainly detected by the IXS measurements. Thus, the above peak broadening (or splitting) may indicate that there are more regions with different elasticities in the SBRs. Also, in this case, since the overall SBRs have elasticity higher than the average value measured by the US technique, WBRs should exist in the glass matrix.

The synchrotron radiation experiments were performed at the SPring-8 with the approval of the Japan Synchrotron Radiation Research Institute (JASRI). This work was partly supported by a Grant-in-Aid for Scientific Research on the Priority Area Investigation of "Materials Science of Bulk Metallic Glasses" from the Ministry of Education, Science, Sports and Culture, Japan.

*tichi@mtl.kyoto-u.ac.jp

[1] F. H. Stillinger, J. Chem. Phys. **89**, 6461 (1988).
[2] G. N. Greaves, J. Non-Cryst. Solids **71**, 203 (1984).
[3] G. P. Johari and M. Goldstein, J. Chem. Phys. **53**, 2372 (1970).
[4] G. P. Johari, J. Chem. Phys. **58**, 1766 (1973).
[5] M. D. Ediger, J. Non-Cryst. Solids **235-237**, 10 (1998).
[6] G. Adam and J. H. Gibbs, J. Chem. Phys. **43**, 139 (1965).
[7] E. Donth, J. Non-Cryst. Solids **53**, 325 (1982).
[8] Y. Hirotsu, T. G. Nieh, A. Hirata, T. Ohkubo, and N. Tanaka, Phys. Rev. B **73**, 012205 (2006).
[9] J. Das, M. B. Tang, K. B. Kim, R. Theissmann, F. Baier, W. H. Wang, and J. Eckert, Phys. Rev. Lett. **94**, 205501 (2005).
[10] T. Ichitsubo, E. Matsubara, S. Kai, and M. Hirao, Acta Mater. **52**, 423 (2004).
[11] T. Ichitsubo, S. Kai, H. Ogi, M. Hirao, and K. Tanaka, Scr. Mater. **49**, 267 (2003).
[12] T. Ichitsubo, E. Matsubara, T. Yamamoto, H. S. Chen, N. Nishiyama, J. Saida, and K. Anazawa, Phys. Rev. Lett. **95**, 245501 (2005).
[13] T. Ichitsubo, E. Matsubara, H. S. Chen, J. Saida, T. Yamamoto, and N. Nishiyama, J. Chem. Phys. **125**, 154502 (2006).
[14] F. Sette, G. Ruocco, M. Krisch, U. Bergmann, C. Masciovecchio, V. Mazzacurati, G. Signorelli, and R. Verbeni, Phys. Rev. Lett. **75**, 850 (1995).
[15] T. Scopigno, G. Ruocco, F. Sette, and G. Monaco, Science **302**, 849 (2003).
[16] J. B. Suck, H. Rudin, H. J. Guntherodt, and H. Beck, Phys. Rev. Lett. **50**, 49 (1983).
[17] A. Meyer, Phys. Rev. B **66**, 134205 (2002).
[18] T. Scopigno, J. B. Suck, R. Angelini, F. Albergamo, and G. Ruocco, Phys. Rev. Lett. **96**, 135501 (2006).
[19] D. Ishikawa, M. Inui, K. Matsuda, K. Tamura, S. Tsutsui, and A. Q. R. Baron, Phys. Rev. Lett. **93**, 097801 (2004).
[20] N. Nishiyama and A. Inoue, Mater. Trans., JIM **37**, 1531 (1996).
[21] T. Ichitsubo, E. Matsubara, H. Numakura, K. Tanaka, N. Nishiyama, and R. Tarumi, Phys. Rev. B **72**, 052201 (2005).
[22] J. M. Pelletier, B. Van de Moortèle, I. R. Lu, Mater. Sci. Eng., A **336**, 190 (2002).
[23] K. Tanaka, T. Ichitsubo, and E. Matsubara, Mater. Sci. Eng., A **442**, 278 (2006).
[24] A. Q. R. Baron, Y. Tanaka, S. Goto, K. Takeshita, T. Matsushita, and T. Ishikawa, J. Phys. Chem. Solids **61**, 461 (2000).
[25] H. H. Demarest, Jr., J. Acoust. Soc. Am. **49**, 768 (1971).
[26] I. Ohno, J. Phys. Earth **24**, 355 (1976).
[27] N. Nishiyama, A. Inoue, and J. Z. Jiang, Appl. Phys. Lett. **78**, 1985 (2001).
[28] B. Fåk and B. Dorner, Institute Laue-Langevin Report No. 92FA008S, 1992 (unpublished).
[29] B. Fak and B. Dorner, Physica B **234**, 1107 (1997).
[30] T. Scopigno, R. Di Leonardo, G. Ruocco, A. Q. R. Baron, S. Tsutsui, F. Bossard, and S. N. Yannopoulos, Phys. Rev. Lett. **92**, 025503 (2004).
[31] B. Ruzicka, T. Scopigno, S. Caponi, A. Fontana, O. Pilla, P. Giura, G. Monaco, E. Pontecorvo, G. Ruocco, and F. Sette, Phys. Rev. B **69**, 100201(R)(2004).
[32] Tullio Scopigno, Giancarlo Ruocco, and Francesco Sette, Rev. Mod. Phys. **77**, 881 (2005).
[33] P. G. Debenedetti and F. H. Stillinger, Nature (London) **410**, 259 (2001).
[34] F. H. Stillinger, Science **267**, 1935 (1995).
[35] K. L. Ngai, Phys. Rev. B **71**, 214201 (2005).
[36] G. P. Johari, J. Non-Cryst. Solids **307-310**, 317 (2002).
[37] E. Duval and A. Mermet, Phys. Rev. B **58**, 8159 (1998).
[38] K. Yoshimoto, T. S. Jain, K. V. Workum, P. F. Nealey, and J. J. de Pablo, Phys. Rev. Lett. **93**, 175501 (2004).
[39] B. Rossi, G. Viliani, E. Duval, L. Angelani, and W. Garber, Europhys. Lett. **71**, 256 (2005).
[40] W. Schirmacher, Europhys. Lett. **73**, 892 (2006).
[41] F. Leonforte, A. Tanguy, J. P. Wittmer, and J.-L. Barrat, Phys. Rev. Lett. **97**, 055501 (2006).
[42] W. Schirmacher, G. Ruocco, and T. Scopigno, Phys. Rev. Lett. **98**, 025501 (2007).